

See discussions, stats, and author profiles for this publication at: <https://www.researchgate.net/publication/225524735>

# Prediction of optical properties of paints

Article in Central European Journal of Physics · September 2007

DOI: 10.2478/s11534-007-0025-6

CITATIONS

9

READS

647

2 authors, including:



Roman Ďuríkovič

Comenius University in Bratislava

99 PUBLICATIONS 316 CITATIONS

SEE PROFILE

Some of the authors of this publication are also working on these related projects:



Optical-Inertial Hybrid Motion Capture Sync System [View project](#)



APCoCoS - Appearance Prediction [View project](#)

## Prediction of optical properties of paints\*

Roman Ďurikovič<sup>1†‡</sup>, Tomáš Ágošton<sup>2§</sup>

<sup>1</sup> Faculty of Natural Sciences,  
University of Saint Cyril and Metod,  
917 01 Trnava, Slovakia

<sup>2</sup> Faculty of Mathematics, Physics and Informatics,  
Comenius University,  
842 48 Bratislava, Slovakia

Received 9 December 2006; accepted 25 April 2007

**Abstract:** The field of predictive rendering concerns itself with those methods of image synthesis which yield results that do not only look real, but are also radiometrically correct renditions of nature, *i.e.*, which are accurate predictions of what a real scene would look like under given lighting conditions. A real coating consists of pigments, effect pigments, clear lacquer and glaze. A novel and unique combination of real parameters that are commonly measured in the industry and a theoretical reflectance model consisting of measurable parameters is required. Here, the authors design perception parameters and put them into well known surface reflection functions such as He and Torrance. The original contributions are the study of the sub-surface scattering of real paint and the prediction of its appearance in rendered images by the proposed model of light reflection beneath the paint surface.

© Versita Warsaw and Springer-Verlag Berlin Heidelberg. All rights reserved.

*Keywords:* appearance, appearance measurements, paint BRDF

*PACS (2006):* 42.15.Dp, 42.30.Lr, 42.25.Hz

## 1 Introduction

How an object looks has been recognized as important in both the field of computer graphics and the appearance industry. The focus of this research is on faithful acquisition

\* Presented at 5-th International Conference Solid State Surfaces and Interfaces, November 19–24, 2006, Smolenice Castle, Slovakia

† E-mail: roman.durikovic@fmph.uniba.sk

‡ Also with Faculty of Mathematics, Physics and Informatics, Comenius University, Slovakia

§ E-mail: tomas.agoston@fmph.uniba.sk

of appearance of surfaces. With this data, objects can be rendered in arbitrary virtual environments, predicting the way the original object would appear. Based on an object's appearance, we can deduce of what materials an object consists. Industry needs to solve the inverse problem — *i.e.*, based on the materials in surface paints, deduce the appearance.

The quantification of appearance by the paint and coatings industries has resulted in a set of appearance measurement standards: tristimulus colorimetry, gloss and haze. *Tristimulus colorimetry* is essentially a measure of diffuse reflection color (shade color). *Gloss* is a measure of the magnitude of the specular reflection, and *haze*, also called glitter, captures the width of the specular lobe. Refer to Fig. 1 for a demonstration of appearance attributes. Gloss and haze are critical for appearance measurement, for knowing how much light is reflected within just a few degrees of the specular direction. Appearance professionals have learned that in many cases, such as automotive metallic and pearlescent paint, only a few key measurements are necessary. Finally, the measurement of gloss, haze, metallic paint and other standardized appearance parameters can all be accomplished with relatively inexpensive measurement instruments.

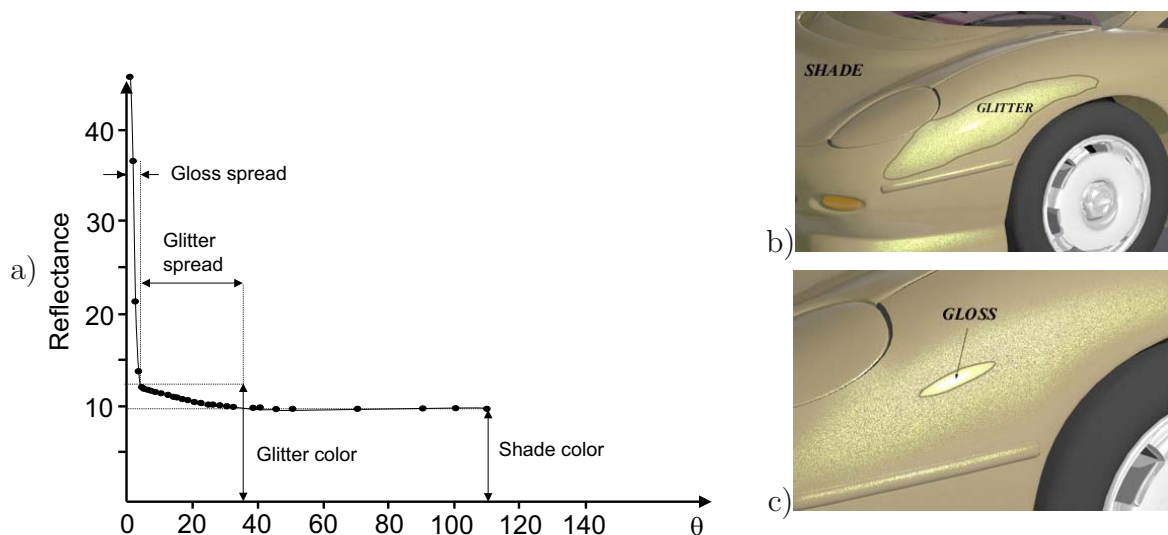


**Fig. 1** Paint appearance attributes: shade, glitter, and gloss. a) Cross-section of measured Bidirectional Reflection Distribution Function (BRDF) of a pearlescent paint at  $\phi = 0^\circ$ . The paint views magnified b) 4 times and c) 8 times [6].

The reaction by computer graphics researchers has been to develop increasingly general models of surface reflection and to build reflection measurement devices. This has led to the use of the Bidirectional Reflection Distribution Function (BRDF) to represent reflection.

Marschner *et al.* [13] proposed an efficient method to measure the isotropic BRDF of materials. A homogeneous sphere sample of the target material is captured with a digital camera in different lighting conditions. The curved sample surface allows the acquisition of many BRDF samples at once and leads to a short acquisition time. Matusik *et al.* [14] built an automatic acquisition system and captured a large database of various materials

including car paints [7]. Ngan *et al.* [15] analyzed how various analytic BRDF models perform when used to fit real measured data. As one result, they found that the physically based BRDF model of Cook and Torrance [3] performed very well, especially with metal-like materials. Günther *et al.* [7] have built their own high-speed BRDF measurement system. A sphere covered with car paint is mounted on the center of a turntable and captured. During acquisition, the light source moves in increments of 1 degree from the point exactly in front of the camera to the position exactly opposite the camera. The Cook–Torrance model with multiple lobes is fit to the measured data for efficient BRDF representation.

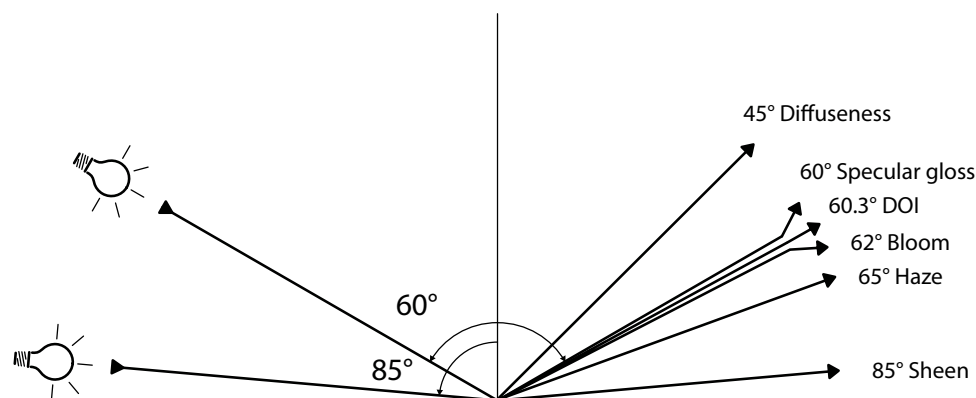


**Fig. 2** Different kinds of gloss are measured as the reflected radiance at specific incident and outgoing directions.

## 2 Gloss

Gloss is defined by the American Society for Testing and Materials (ASTM) to be “the angular selectivity of reflectance, involving surface-reflected light, responsible for the degree to which reflected highlights or images of objects may be seen as superimposed on a surface” [1]. We can differentiate several types of gloss measured at specific angles as illustrated in Fig. 2.

**Specular gloss:** Specular gloss is measured for the exact mirror direction.

**Sheen:** Sheen measures the shininess at grazing angles.

**Luster:** Contrast gloss or luster is a relative measure between specular reflecting areas and other areas.

**Haze:** Bloom and haze describe the milky appearance, adjacent to specular reflections.

**DOI:** Distinctness-of-image gloss measures the sharpness of mirror images, relevant for high-gloss surfaces.

**Diffuseness:** In addition to the gloss, one may express the diffuseness of a high-gloss surface by a measurement far off the mirror direction.

ASTM Method D523-39, Test for *Specular Gloss*, measures the light reflected in the specular direction off the sample surface, 60 degrees down from surface normal. A high gloss surface will reflect most light in the specular direction while a surface with low

gloss will reflect most of its light in directions other than specular. The numerical gloss value,  $G$ , assigned to a surface typically ranges from 100 (high gloss) to 0 (low gloss). An example of a low gloss surface is a Lambertian surface. Part of the standard are two more angles, 85 degrees from normal, which measures specular gloss at grazing angles (called sheen) and 20 degrees which measures specular gloss at near normal angles [1].

ASTM E430 offers measurements of the perceived haziness of surfaces. The haze value is a measure of the similarity between the pure specular reflection (measured with 30 degree gloss) and off-specular reflection (measured either 2 or 5 degrees off specular). The notation used for the measured value of haze,  $H$ , is an increasing numerical value associated with increasing haziness.

ASTM E430 Test Method A defines the distinctness-of-image gloss measurements. These measurements compare the light reflected directly in the specular direction to that reflected in the slightly off-specular direction. The angle of offset is essentially a mere 0.3 degrees. This is to mimic the keen discrimination of the human visual system for detecting the sharpness of the reflection of an object in a highly reflective surface. The quantity measured is  $G_{doi}$ , a larger value of  $G_{doi}$  corresponding to a more distinct image.

## 2.1 Industry appearance measurement devices

Spectrophotometers are used to objectively measure and validate colors, excluding the possibility of metamerism experienced by a human observer. The full visible spectrum of reflectance of the material sample is measured. This is done by dispersing the gathered light beam into spectral colors (by a prism or grating) and projecting the colors onto a photodiode array. Each part of the array measures a different wavelength of light. Spectrophotometers are manufactured in different optical geometry configurations, making them proper for various fields of usage — see Fig. 3.

Recently, the industry has introduced two types of multi-angle spectrophotometers which are suitable for measuring optical attributes of goniochromatic car paints, but which are also considerably expensive. The first type is based on unidirectional lighting with multiple viewing angles (refer to Fig. 3). The second type overcomes this drawback and illuminates the sample in ring shapes, but the radiance is measured only in the normal direction.

## 3 Data acquisition

We use two approaches to build up a database of paint and coatings appearance attributes. In our first approach we will utilize industry standard appearance measurement devices, which are used to determine the quality and acceptability of a variety of product finishes. Current industry standards reduce the measurement results to only a few samples, which is not enough to directly reproduce any reasonable BRDF by sampling. However our goal is to investigate the possibility of using these devices as validation tools for our analytic BRDF models for car paints.

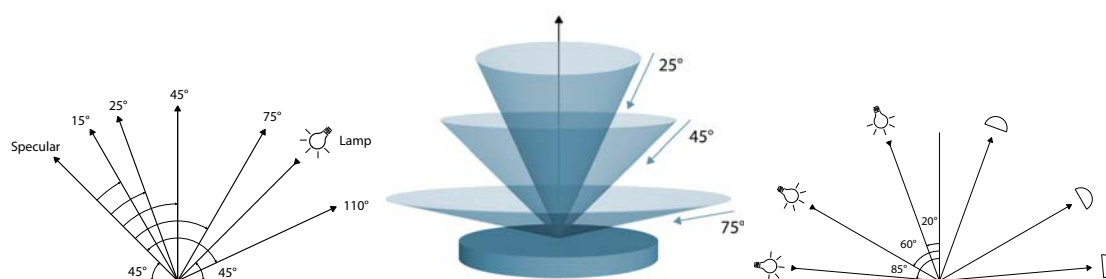


**Fig. 3** Geometry configuration. Right: Spectrophotometer multi-angle viewing geometry. Center: Spectrophotometer multi-angle ring shaped lighting. Left: Glossmeter geometry — the illumination angle is equal to the viewing angle.

We use a standard glossmeter and colorimeter. The glossmeter conforms to standards [10] and is able to measure gloss and reflectance under the geometry of three angles: 20°, 60°, 85° (see Fig. 3). The colorimeter measures the tristimulus color of the diffusely lighted surface viewed at 8° from the normal direction with a  $d/8$  geometry.

## 4 Goniochromatic paints

The color of an opaque dielectric is typically modeled with Lambertian reflectance — *i.e.*, the color is considered constant with respect to the viewing angle. However, goniochromatic materials such as metallic and pearlescent paints change color with viewing angle.

Metallic paints are produced by combining metallic platelets with colored particles (see the paint cross section on Fig. 4). In a dry paint, the platelets are oriented nearly parallel to the surface and therefore most of the light is reflected near the specular direction. The colored particles tint the light through selective absorption resulting in a bright color in the near specular direction falling off to a dark color away from specular. This change in lightness is termed flop, also called flip/flop. The metallic flakes are fifty times bigger than the colored pigments. Their size ranges from 5 to 45  $\mu\text{m}$  and their thickness from 0.1 to 1  $\mu\text{m}$ .

Pearlescent paint combines colored particles with small flakes of mica coated with thin layers of metal oxide which both reflect and transmit incident light. These thin layered platelets cause interference and thus the flop phenomena in pearlescents involves variation in all three coordinates of the color space rather than simply lightness.

It would be a very restrictive approach to represent the appearance only by the gloss measured for a surface.

## 5 Paint appearance simulation

We chose to simulate the stacking of pigmented layers with Kubelka and Munk's theory [11]. This allows us to take into account the local influence of subsurface scattering on the pigmented layer applied upon the primer layer. Kubelka and Munk's theory is con-

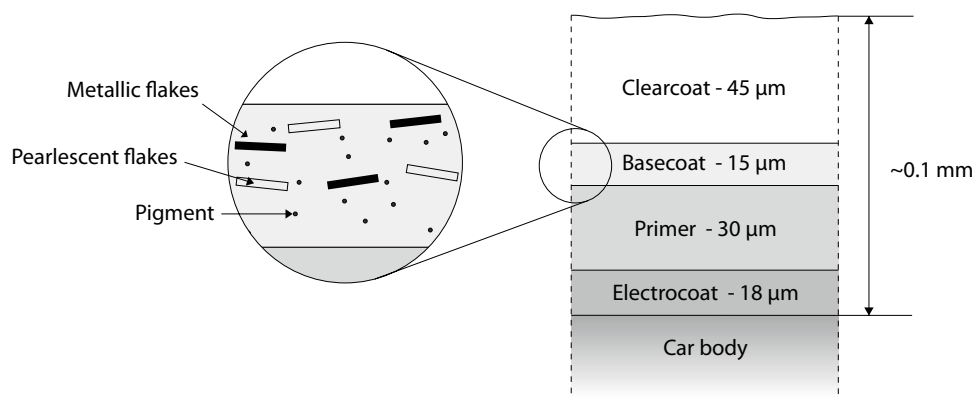


**Fig. 4** Real car paint structure.

sidered as a good evaluation of the reflectance in the normal direction to the surface while it assumes that the incident and the outgoing light flux are diffuse. The Cook–Torrance model [3] is physically based and has shown to perform well with many materials [15]. In its multi-lobe form, the Cook–Torrance BRDF can be used as a reflectance model, including all components such as clear coat reflectance, pigment layer reflectance, and reflectance of metallic and pearl flakes. The composite BRDF  $f_r$  of the car coating for given incoming direction  $\omega_i$  and outgoing direction  $\omega_o$  can be expressed:

$$f_r(x, \omega_i, \omega_o) = \rho + \tau \left( (1 - A_m - A_p) R_l + A_m \frac{R_m D_m G}{\pi (\mathbf{n} \circ \omega_i)(\mathbf{n} \circ \omega_o)} + A_p \frac{R_p D_p G}{\pi (\mathbf{n} \circ \omega_i)(\mathbf{n} \circ \omega_o)} \right), \quad (1)$$

where  $\rho$  and  $\tau$  are the reflectance and transmittance of the clear coat, respectively;  $A_m$  and  $A_p$  are the area ratio of visible metallic and pearlescent flakes, respectively;  $R_l$  is the reflectance of the pigmented layer;  $R_m$  and  $R_p$  are the reflectance of metallic and pearlescent flakes embedded in the pigmented layer, respectively;  $D_m$  and  $D_p$  are the angular distributions of the metallic and pearlescent flakes, respectively; and  $G$  is the geometric attenuation factor as defined by the Cook and Torrance model. The normal vector to the painted surface is denoted as  $\mathbf{n}$ .

## 5.1 Clear coat

The clear coat is a 20  $\mu\text{m}$  thick layer of resin that has the same index of refraction as the layer with pigment and flakes. The only important factor here is the interface between the air and clear coat that is simulated by Fresnel's formulae for dielectrics. Fresnel formulae can be used to compute  $\rho$  and  $\tau$  for given incoming direction  $\omega_i$  and transmitted direction  $\omega_t$ .

Let  $r_\perp$  and  $r_\parallel$  be the reflected amplitude ratios of the field perpendicular and parallel to the plane spanned by  $\omega_i$  and  $\mathbf{n}$ . Accordingly,  $t_\perp$  and  $t_\parallel$  denote the ratios of the transmitted amplitudes. Those can be calculated as

$$r_\perp = \frac{\eta_1(\mathbf{n} \circ \omega_i) - \eta_2(\mathbf{n} \circ \omega_t)}{\eta_1(\mathbf{n} \circ \omega_i) + \eta_2(\mathbf{n} \circ \omega_t)}, \quad r_\parallel = \frac{\eta_2(\mathbf{n} \circ \omega_i) - \eta_1(\mathbf{n} \circ \omega_t)}{\eta_2(\mathbf{n} \circ \omega_i) + \eta_1(\mathbf{n} \circ \omega_t)},$$

$$t_{\perp} = \frac{2\eta_1(\mathbf{n} \circ \boldsymbol{\omega}_i)}{\eta_1(\mathbf{n} \circ \boldsymbol{\omega}_i) + \eta_2(\mathbf{n} \circ \boldsymbol{\omega}_t)}, \quad t_{\parallel} = \frac{2\eta_1(\mathbf{n} \circ \boldsymbol{\omega}_i)}{\eta_2(\mathbf{n} \circ \boldsymbol{\omega}_i) + \eta_1(\mathbf{n} \circ \boldsymbol{\omega}_t)}.$$

The reflectance and transmittance of the clear coat can then be calculated as

$$\rho = \frac{1}{2}(r_{\perp}^2 + r_{\parallel}^2) \text{ and } \tau = \frac{\eta_2(\mathbf{n} \circ \boldsymbol{\omega}_i)}{\eta_1(\mathbf{n} \circ \boldsymbol{\omega}_t)} \frac{1}{2}(t_{\perp}^2 + t_{\parallel}^2). \quad (2)$$

Note that when light travels through a material of index  $\eta_1$  and hits the surface of some medium with lower index  $\eta_2$  ( $\eta_1 > \eta_2$ ), like from glass to air, the transmittance  $\tau$  will be zero if the incident angle  $(\mathbf{n} \circ \boldsymbol{\omega}_i)$  exceeds the critical angle. The input parameter  $\eta_2 = \eta_{cc}$  is the index of refraction of the clear coat varying between 1.4 and 1.6, depending on the resin, and  $\eta_1 = 1$  for air.

## 5.2 Reflectance of pigmented layer

The reflectance  $R_l$  of the pigmented layer painted above the prime layer can then be written according to Kubelka and Munk's theory:

$$R_l = \frac{(1 - R_{\infty})(R_g - R_{\infty}) - R_{\infty}(R_g - \frac{1}{R_{\infty}}) \exp \left[ SX(\frac{1}{R_{\infty}} - R_{\infty}) \right]}{(R_g - R_{\infty}) - (R_g - \frac{1}{R_{\infty}}) \exp \left[ SX(\frac{1}{R_{\infty}} - R_{\infty}) \right]}, \quad (3)$$

where  $R_g$  is the reflectance of the primer and  $X$  the thickness of the pigmented layer, both known from measurements. The reflectance of an infinitely thick pigmented layer is

$$R_{\infty} = 1 + \frac{K}{S} - \sqrt{\frac{K^2}{S^2} + 2\frac{K}{S}}, \quad (4)$$

where  $K$  and  $S$  are respectively the absorption and the scattering of the layer, depending on wavelength.  $K$  and  $S$  can be derived from measurements by inverting the Kubelka and Munk's formulae. Given  $R_w(r, g, b)$  of the pigmented layer of thickness 1 over a white background, and reflectance  $R_b(r, g, b)$  of the pigmented layer of thickness 1 over a black background, we compute  $K$  and  $S$  [4]. Having several pigments in this layer we need to know the respective concentration  $C_i$  of pigments and parameters  $K_i$  and  $S_i$  for each pigment. Therefore the ratio  $K/S = (\sum_i C_i K_i) / (\sum_i C_i S_i)$ .

The pigmented layer is a model for opaque tints. Next, we extend this model to generate the range of effects of metallic and pearlescent coatings.

## 5.3 Reflectance of metallic flakes

Although in a dry paint the flakes are oriented nearly parallel to the surface, we take into account the shadowing effect by flakes and we propose to use Cook and Torrance's model to evaluate the composite reflectance of metallic flakes in a pigmented layer. Refer to the third term in Eq. (1).

In order to simulate metallic flakes immersed within the pigmented layer, we calculate a reflectance  $\rho_m$  of a single metallic flake from Fresnel formulae. Since a metal is a



conductor, we take  $\eta_2$  equal to the complex index of refraction of the metal and  $\eta_1$  as the index of refraction of the medium in which the flakes are embedded [see Eq. (2)].

A metallic flake is a small mirror reflecting the light that will travel through the pigmented layer, the distance depending on the depth of the flake. Letting  $X'$  be the average depth of the visible flakes, we can use mixing by Kubelka and Munk's model to derive the reflectance of the pigmented layer with thickness  $X' < X$  that is above the metallic flake:

$$R_m = \frac{(1 - R_\infty)(\rho_m - R_\infty) - R_\infty(\rho_m - \frac{1}{R_\infty}) \exp [SX'(\frac{1}{R_\infty} - R_\infty)]}{(\rho_m - R_\infty) - (\rho_m - \frac{1}{R_\infty}) \exp [SX'(\frac{1}{R_\infty} - R_\infty)]}. \quad (5)$$

Unfortunately, we cannot measure the depth  $X'$  and it is not available from manufacturers.

## 5.4 Pearlescent flakes

As for metallic flakes, Cook and Torrance's model is used to simulate the random orientation of flakes in the pigmented layer. A visible area ratio is applied to weight the reflectance of the flakes, as only a few of them are visible through the layer. Refer to the last term in Eq. (1).

We must calculate the reflectance  $\rho_p$  of a single pearlescent flake and then immerse it into the pigmented layer. These flakes are generally composed of a mica platelet coated with a titanium dioxide thin film. The thickness of the thin film determines the color of the pigment. We can assume that the flakes consist of three layers forming interferential systems.

Let us first derive the composite reflectance,  $\rho_p$ , and transmittance,  $\tau_p$ , of the three-layered film system of a pearlescent flake calculated by an iterative method from the last layer to the first [9]:

$$\begin{aligned} \rho_0 &= r_4, & \tau_0 &= t_4, \\ \text{for } j &= 3, \dots, 1 & \rho_{3-j+1} &= \frac{r_j + \rho_{3-j} e^{2i\varphi_j}}{1 + r_j \rho_{3-j} e^{2i\varphi_j}}, & \tau_{3-j+1} &= \frac{t_j \tau_{3-j} e^{i\varphi_j}}{1 + r_j \rho_{3-j} e^{2i\varphi_j}}, \end{aligned} \quad (6)$$

where  $i$  denotes the imaginary number,  $r_j$  and  $t_j$  are the reflectivity and transmissivity at a boundary between the  $(j-1)$ -th and  $j$ -th layers, respectively, and these coefficients are obtained by Fresnel formulae. Note that  $r_4$  and  $r_1$  are calculated at the boundary between titanium dioxide thin film and resin.  $\varphi_j = \frac{1\pi d_j}{\lambda} \sqrt{\eta_j^2 - \eta_{j-1}^2} \sin^2 \theta_{j-1}$  is the phase difference between boundaries of the  $j$ -th layer. Here  $d_j$  is the thickness of the  $j$ -th layer;  $\theta_{j-1}$  is the angle of the incoming ray at the interface between the  $(j-1)$ -th layer and the  $j$ -th layer of the flake.

$\rho_j$  and  $\tau_j$  are the composite reflectivity and transmissivity at a boundary between the  $j$ -th and  $(j+1)$ -th layers, respectively. On the other hand, the reflectance and transmittance represent ratios of energies of reflected and transmitted light, respectively, and they are obtained by the square of the absolute value of the reflectivity and transmissivity.

Finally, the composite reflectance,  $\rho_p$ , and transmittance,  $\tau_p$ , of a pearlescent flake are calculated analogously to Eq. (2):

$$\rho_p = \frac{1}{2}(\rho_{3,\perp}^2 + \rho_{3,\parallel}^2), \quad \tau_p = \frac{\eta_4(\mathbf{n} \circ \boldsymbol{\omega}'_i)}{\eta_0(\mathbf{n} \circ \boldsymbol{\omega}'_t)} \frac{1}{2}(\tau_{3,\perp}^2 + \tau_{3,\parallel}^2), \quad \text{for real } \eta_4, \quad \tau_p = 0 \text{ for complex } \eta_4, \quad (7)$$

where  $\eta_0$  and  $\eta_4$  denote refractive indices of the 0-th and 3-rd layers, respectively, and the other arguments are illustrated in Fig. 4. It is important to notice that the mica platelet is too thick to produce interference between rays exiting from the first and second thin films.

A pearlescent flake is embedded into a pigmented medium. The pearlescent flake reflects light after interference in the flake back, and the light travels through the pigmented layer a distance depending on the depth of the flake. Letting  $X''$  be the average depth of the visible flakes, we can use mixing by Kubelka and Munk's model to derive the reflectance of the pigmented layer with thickness  $X'' < X$  that is above the pearlescent flake:

$$R_p = \frac{(1 - R_\infty)(\rho_p - R_\infty) - R_\infty(\rho_p - \frac{1}{R_\infty}) \exp[SX''(\frac{1}{R_\infty} - R_\infty)]}{(\rho_p - R_\infty) - (\rho_p - \frac{1}{R_\infty}) \exp[SX''(\frac{1}{R_\infty} - R_\infty)]}. \quad (8)$$

## 6 Validation of BRDF by appearance measurements

Westlund and Meyer [8] presented a correspondence between BRDF model parameters and standard appearance measurements. A virtual light meter was constructed for this purpose. In the same way that various gloss meters give control over surface reflection properties, a virtual light meter can give control over BRDF model parameters to the computer graphics appearance designer.

The method is essentially a numerical quadrature of the specified analytical BRDF model over an adaptively subdivided source and receptor aperture in order to compute a final standard appearance value such as specular gloss, haze, and distinctness-of-image. The customizable parameters include the size and locations of the source and receptor apertures, the specular angle, the surface orientation, and the surface reflection model.

The ASTM gloss and haze measurements are designed to work with surfaces exhibiting Fresnel effects. Thus, any BRDF model which includes Fresnel reflection can be used without modification in the virtual haze and gloss meter as we did with the Cook–Torrance model.

## 7 Results

Summary of the parameters used in our paint model:

- **Pigmented Layer**
  - (1) the spectral reflectance of the primer
  - (2) the thickness of the layer
  - (3) the respective concentration of pigments

- (4) parameters  $K$  and  $S$  for each pigment
- **Metallic Flakes**
  - (1) the kind of flakes (complex index of refraction of metal)
  - (2) the angular distribution of flakes (close to  $0^\circ$ )
  - (3) the area ratio where flakes are visible
  - (4) the average depth of visible flakes
- **Pearlescent Flakes**
  - (1) the thin film thickness
  - (2) the angular distribution of flakes (close to  $0^\circ$ )
  - (3) the area ratio where flakes are visible
  - (4) the average depth of the visible flakes

Measurement devices-gloss meters and colorimeters — can be used to validate the basic properties of BRDF and to set the  $\rho$ ,  $\tau$  and  $R_l$  parameters of our global BRDF model to fit the measured data.

Figure 5 shows examples rendered by the proposed method. We employed a Cook–Torrance model to define reflection properties of the rough surfaces, and the spectral distribution of light sources is set to D65. The paint shown on Figure 5(a) is a blue pigmented paint with clear coat thickness  $0.45\ \mu\text{m}$ , index of refraction 1.5, binder thickness 0.15, pigment concentration 0.4,  $K = (1.52, 0.32, 0.25)$ ,  $S = (0.06, 0.25, 0.4)$ , and reflectance of primer  $R_g = (0.7, 0.7, 0.7)$ . In Figure 5(b), the metallic flakes were added with the following parameters: angular distribution  $0.25^\circ$ , visible area ratio 0.4, and flake’s index of refraction  $(0.93 + i6.33)$ . Finally, in Figure 5(c), we have added pearlescent flakes with angular distribution  $0.35^\circ$ .



(a) Blue pigment      (b) added metallic flakes      (c) added pearlescent flakes

**Fig. 5** “Cerulean Blue” car paint.

## 8 Conclusions

Standards for measurement of pigment paints have been summarized; unfortunately, the standard measurements for effect paints have as yet to be specified. Gloss and haze in reflection models can be determined using inexpensive measurement instruments. This

makes it possible to model the appearance of an existing object by making a few simple measurements. We proposed the BRDF model of a single layered paint consisting of several pigments, and metallic and pearlescent flakes. A surface with metallic or pearlescent paints can be rendered using as few as four data values: one gloss measurement in the specular direction and colorimetric measurements in three given directions opposite to the specular one.

Further studies are necessary to extend this model to be based more on measurable parameters available from industry devices.

## Acknowledgment(s)

The authors thank Michal Klempai for rendering the images, and Konstantin Kolchin and Karol Myszkowski for their ongoing support of this project. This research was supported by a Marie Curie International Reintegration Grant within the 6-th European Community Framework Programme.

## References

- [1] ASTM D 523-89:1999, *Standard Test Method for Specular Gloss, Vol. 06.01 of Annual Book of ASTM Standards*.
- [2] C.S. McCamy: “Observation and Measurement of the Appearance of Metallic Materials. Part I. Macro Appearance”, *Col. Res. App.*, Vol. 21, (1996), pp. 292–304.
- [3] R.L. Cook and K. E. Torrance: “A Reflectance Model for Computer Graphics”, *Acm. T. Graphic.*, Vol. 1, (1982), pp. 7–24.
- [4] Cassidy J. Curtis, Sean E. Anderson, Joshua E. Seims, Kurt W. Fleischer and David H. Salesin: “Computer-Generated Watercolor”, In: *Proceedings of SIGGRAPH 97*, ACM Press, 1997, pp. 421–430.
- [5] R. Ďurikovič, K. Kolchin and S. Ershov: “Rendering of Japanese Artcraft”, In: I.N. Alvaro and Ph. Slusallek (Ed.): *Proceedings of the EUROGRAPHICS short presentations*, Blackwell Publishers, UK, 2002, pp. 131–138.
- [6] S. Ershov, R. Ďurikovič, K. Kolchin and K. Myszkowski: “Reverse Engineering Approach to Appearance-based Design of Metallic and Pearlescent Paints”, *The Visual Computer*, Vols. 8–9, (2004), pp. 586–599.
- [7] J. Günther, T. Chen, M. Goesele, I. Wald and H.-P. Seidel: “Efficient Acquisition and Realistic Rendering of Car Paint”, In: *Vision, Modeling, and Visualization*, Akademische Verlagsgesellschaft Aka GmbH, Berlin, 2005, pp. 487–494.
- [8] Harold B. Westlund and Gary W. Meyer: “Applying Appearance Standards to Light Reflection Models”, In: *Proceedings of SIGGRAPH 2001*, ACM Press, New York, USA, 2001, pp. 501–510.
- [9] H. Hirayama, K. Kaneda, H. Yamashita and Y. Monden: “An Accurate Illumination Model for Objects Coated with Multilayer Films”, *Comput. Graph.*, Vol. 25, (2001), pp. 391–400.

- [10] ISO 2813:1994, *Paints and varnishes - Determination of specular gloss of non-metallic paint films at 20 degrees, 60 degrees and 85 degrees*.
- [11] P. Kubelka and F. Munk: “Ein beitrag zur optik der farbenstriche”, *Zurich Tech. Physik*, Vol. 12, (1931), pp. 593–561.
- [12] J. Lawrence, A. Ben-Artzi, C. DeCoro, W. Matusik, H. Pfister, R. Ramamoorthi and S. Rusinkiewicz: “Inverse Shade Trees for Non-Parametric Material Representation and Editing”, *Acm. T. Graphic.*, Vol. 25, (2006), pp. 735–745.
- [13] S.R. Marschner: *Inverse Rendering for Computer Graphics*, Thesis (PhD), Cornell University, 1998.
- [14] W. Matusik, H. Pfister, M. Brand and L. McMillan: “A Datadriven Reflectance Model”, *Acm. T. Graphic.*, Vol. 22, (2003), pp. 759–769.
- [15] A. Ngan, F. Durand and W. Matusik: “Experimental Validation of Analytical BRDF Models”, In: *ACM SIGGRAPH - Sketches and Applications*, ACM Press, 2004, pp. 129–138.
- [16] G. Rosler: “Multigeometry color measurements of effect surfaces”, *Die Farben*, Vol. 37, (1990), pp. 111–121.
- [17] H.J.A. Saris, R.J.B. Gottenbos and H. van Houwelingen: “Correlation between visual and instrumental colour differences of metallic paint films”, *Col. Res. App.*, Vol. 15, (1990), pp. 7–24.